International Journal of Control and Automation
Vol.8, No.8 (2015), pp.373-384
http://dx.doi.org/10.14257/ijca.2015.8.8.35

An Image-Based Approach for Modeling the Copper Particle Uniformity in Formulation Design of Copper-Coated Graphite

Hai-Ming Liu and Zhang-Can Huang

School of Science, Wuhan University of Technology, Wuhan 430070, China

Abstract

To investigate the uniformity of copper particles in formulation design of copper-coated graphite, a quadrat-based method was presented with the image processing. Firstly, the particles were located by the foreground and background clustering algorithm. Then, an improved uniformity quantification model was established using the size and position of the particles. The findings based on the experimental results of the proposed method are as follows: the method is an effective way to quantify the uniformity by comparing with the human visual achievement; the quadrat number should be low to preserve the high performance of the method; at last, it is reasonable to use the mean uniformity in formulation design.

Keywords: *copper-coated graphite, spatial uniformity, quadrat-based uniformity model, particle distribution, formulation design*

1. Introduction

In formulation design of composite materials, the spatial distribution of particles or components highly affects the quality of the materials. The quality of materials is much better due to the high uniformity of the particles. As for copper-coated graphite, electrical conductivity, thermal conductivity, lubricity and mechanical strength are influenced by the uniformity of copper particle distribution [1]. Since copper-coated graphite compositions possess the characteristics of both copper and graphite, they are used in many fields such as electrode material and conductive material [2-4]. Meanwhile, despite the inconvenient and inaccurate of human perceptions, the uniformity of copper particles is commonly estimated from human visual inspection in formulation design. Currently, there are a few literatures on quantifying the uniformity of particles in formulation design. Hence, it is a challenge task to design a suitable uniformity quantification model. The following section lists the most popular uniformity evaluation approaches.

Most quantitative automatic uniformity calculation methods are based on spatial point pattern. The hypothesis of these methods is that the particles could be considered as dimensionless points due to their small size compared with the study regions. The metrics of quantifying the uniformity based on spatial point pattern can mainly be categorized into three groups: quadrat-based methods, distance-based methods and other methods [5-6]. Firstly, quadrat-based methods divide the study region into a number of minor grids, which is called quadrats. Then, the number of particles in each quadrat is counted. Finally, the mathematical model of counts is employed to calculate the uniformity of particles. However, as only the counts are used, the spatial information is lost. Distance-based methods, containing F-function, G-function, L-function, etc., focus on using the distance between points to describe the uniformity. Most of these methods use the distance between the nearest neighbors. The uniformity is quantified by the characteristics of the distance. As it is indicated by Cressie [7], these methods utilize more spatial information than quadrat-based method, but how to choose the distance is arbitrary. Other methods, including projection index method [8], coefficient of variation exponential power method [9], etc., quantify the uniformity from other aspects. All these methods are under the

ISSN: 2005-4297 IJCA

aforementioned assumption. Nevertheless, according to the study region, such as the evaluation of asphalt mixture homogeneity [10], the assumption that particles can be treated as points is unsuitable, which implies that the particle size should be taken into consideration.

To improve the disadvantages of current methods, a novel automatic uniformity quantification model was presented, in which the spatial information was used as one index in the model. Firstly, the copper particles should be located for automatic measuring the uniformity. Hence, a clustering algorithm was employed to inspect the copper particles. Thereafter, the size, number and position of copper particles could be captured. On one hand, global Shannon entropy (GSE) was employed to describe the uniformity with the particle size and number. On the other hand, the particle position is formulated with the proposed method by considering the dispersion of particles. Experiments were implemented based on the proposed model. Quadrat number has a vital influence on the uniformity. By combining the GSE model and the proposed position-based model, the results were more reasonable than just using a single model. Our approach could be easily extended to other uniformity assessments, such as quality control in manufacturing.

The rest of this paper is organized as follows. Section 2 shows the procedure of particle location. Section 3 analyses the factor influencing the uniformity and establishes the model of uniformity quantification. Section 4 reports our experiments study. Section 5 concludes our works and points out the future study directions.

2. Particle Locations

Particle detection based on image processing is extensively used in many studies [11]. Frequently, the image is first converted to gray image. Then, a bianrization method is employed the binary the image. The particle is detected after the noise suppression. Fast and accurate detection algorithm is necessary to analysis the quality of the particles.

In this study, particle location is the basis for uniformity calculation. It means the results of image-processing critically affect the performance of uniformity quantification, and the more accurate the particle located, the better the uniformity quantified. To detect the particles, the image is divided into some unoverlapping sub-images. Then, a thresholding algorithm is used to detect the particles. After that, a morphological transformation is employed to fill up the gaps and suppress the noise. At last, area filtering is used to remove the obvious noise. Figure 1 shows the flowchart of the steps of particle location.

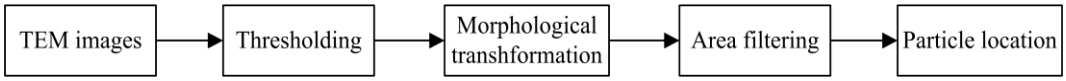

Figure 1: Steps of Particle Location

2.1. Thresholding

There are various methods to detect objects in an image, in which thresholding method is a simple but effective way to separate objects from the background. About forty thresholding methods are studied by Sezgin [12], and the research indicates that there is no universal thresholding method suiting for all images.

An example of copper-coated graphite TEM images is shown in Figure 2. The small black regions (see the red rectangle) in the image are copper particles, while the others are continuous graphite sheet (see the blue rectangle). The size of copper particles on the surface of copper-coated graphite approximately comes to be 1-50nm. The entire image is unclear and inadequate contrast. So it is difficult to locate the copper particles in the image with just one threshold. In this case, the image is divided into $M \times N$ sub-images. In each sub-image, the method proposed by Ridler [13] is utilized to get the binary image.

The iterative algorithm is as following:

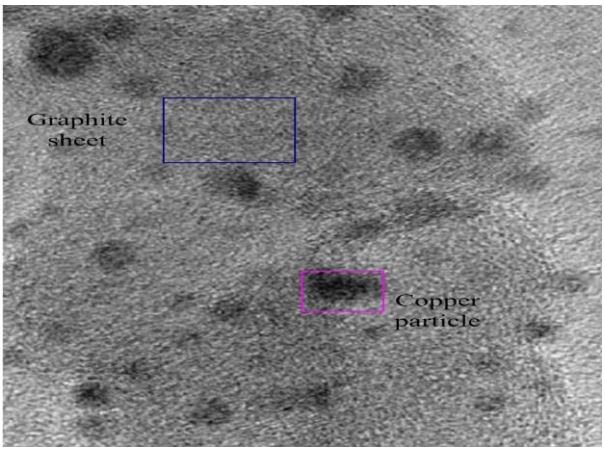

Figure 2: The TEM Image of Copper-Coated Graphite

Step1. Set $m_1=0$, $m_2=0$, $th^0=(m_1+m_2)/2$.

Step2. At step k, compute m_1 and m_2 as the mean background and object gray-level, where $f(x, y)$ is the pixel value at point (x, y), $N_1$and N_2 are the number of background and object pixels, respectively. The threshold th^k is determined by the equation in Step 3. The formula of m_1 and m_2 can be written as follows:

$$m_1 = \frac{\sum_{f(x,y)<th^k} f(x,y)}{N_1} \quad , \quad m_2 = \frac{\sum_{f(x,y)\geq th^k} f(x,y)}{N_2} \tag{1}$$

Step3. Update th^{k+1}

$$th^{k+1} = (m_1 + m_2)/2 \tag{2}$$

Step4.If $th^{k+1}= th^k$, halt and th^{k+1} denotes the best threshold, otherwise return to Step 2.

2.2. Morphological Transformations

After binarization, TEM image contains amount of noise, which should be filtered. Herein, the noise is filtered from two aspects, including morphological transformations and area filtering. Copper particles become black regions after thresholding, and the color should be inversed, so the particles are located as white regions. The formula is:

$$g(x,y) = \begin{cases} 1 & if \ \ f(x,y) = 0 \\ 0 & esle \end{cases} \tag{3}$$

Then, morphological transformations are taken to filter the image. The formula can be written as follows:

$$G(x,y) = [g(x,y) \bullet SE1] \circ SE2 \tag{4}$$

Where, $\bullet$ and $\circ$ are morphological closing and opening. *SE1* and *SE2* are isotropic structuring elements. Closing and opening are used to eliminate specific image details smaller than the structuring element, while the global shape of the objects is not distorted [14]. Closing connects objects that are close to each other, fills up small holes and smoothes the object outline by filling up narrow gulfs. Opening removes the minor objects, separates the objects that are connected with limited points and also smoothes the object outline. Size of structuring element, which is chosen based on the specific

problems has an influence on the object size.

2.3. Area Filtering

The objects contain some particles, which are so tiny that they cannot be the actual copper particles after morphological transformation. Thus, area filtering is employed to be carried out. By setting area threshold S_0, the particles are filtered by the following formula:

$$G(x,y)=\begin{cases}1 & if\ S(x,y)>S_0\\ 0 & if\ S(x,y)\le S_0\end{cases} \tag{5}$$

Where, *S(x,y)* is the area of region containing point *(x,y)*. The area in an image is the number of pixels constituting the region. Minor holes in detected particles are filled up with a flood-fill method.

With the image processing, the copper particle size, number and position can be obtained, which is used to evaluate the uniformity of the copper particles. Based on the database, the uniformity quantification model can be established.

3. Uniformity Quantifications

Quadrat-based methods are commonly employed to quantify the particle uniformity. However, such methods use no spatial information. A novel index, which is called as the local distance index, the distance between quadrat center and average particle centroid is used to quantify the uniformity. Three uniformity indices, including particle number, particle size and local distance index, are specified to describe the particle uniformity, respectively. The three indices are listed in follows.

Number index characterizes the uniformity with the counts in each quadrat. The uniformity is better if the counts in each quadrat are similar, which means the number index is lager.

Size index characterizes the uniformity with the particle size in each quadrat. The larger the size index is, the better the uniformity is. The case in uniformity evaluation through the size index is the same as using number index.

Local distance index characterizes the uniformity with the distance between quadrat center and particles average centroid in each quadrat. The index describes the symmetry about the quadrat center. The larger the distance is, the more uneven the particles are.

3.1. Particle Number and Area Index

Global Shannon entropy (*GSE*) whose value ranges from 0 to 1 is a commonly used entropic measure and has been applied in many fields, such as Camesasca [15] and Guida [16] to assess mixing quality in material processing. Under complete spatial randomness, the probability of particles in each quadrat is the same, and thus *GSE=1*. A small *GSE* value indicates a substantial departure from uniform meaning a low degree of uniformity. *GSE* describes the average self-information obtained from the sum of the self-information of each possible event weighted by the probability of occurrence of the event itself. It can be expressed as follows:

$$GSE(\mathbf{x})=(\sum_{i=1}^{q} p_i \log\frac{1}{p_i})/\log q \tag{6}$$

$$p_i = x_i \Big/ \sum_{i=1}^{q} x_i \tag{7}$$

Where, q is the number of quadrats. In other words, TEM image is divided into $\sqrt{q}\times\sqrt{q}$ quadrats. $\boldsymbol{x}=(x_1, x_2, \ldots, x_q)$signifies the index used to calculate the particle uniformity, and it is a q dimensional vector. p is the probability of index in each quadrat. The formula includes the case *0log1/0*, so it is justified by the limit:

$$\lim_{p\to 0}(p\log\frac{1}{p})=0 \tag{8}$$

According to the counts and area captured in each quadrat, the uniformity can be calculated with formula $I_1=GSE(\boldsymbol{n})$ and $I_2=GSE(\boldsymbol{s})$, where $\boldsymbol{n}=(n_1, n_2, \ldots, n_q)$, $\boldsymbol{s}=(s_1, s_2, \ldots, s_q)$. n_i and s_i represent the particle number and area in quadrat i. I_1 and I_2 describe the uniformity using the particle number and area, respectively.

3.2. Local Distance Index

I_3 denotes the uniformity evaluated with the DCC. The particle average centroid in quadrat I is:

$$x_i=\frac{1}{n_i}\sum_{j=1}^{n_i}x_j \qquad y_i=\frac{1}{n_i}\sum_{j=1}^{n_j}y_j \tag{9}$$

Where, (x_j, y_j) is the jth particle centroid in quadrat i, n_i is the particle number in this quadrat.

The quadrat center is (X_i, Y_i), so the distance between average centroid and center of particles is：

$$d_i=\sqrt{(x_i-X_i)^2+(y_i-Y_i)^2}, i=1,2,\ldots,q \tag{10}$$

If the particle distribution is complete randomness, the distance distribution should also be randomness. D_i is the maximum distance between centroid and center in quadrat i. Uniformity in quadrat i can be quantified in the following:

$$\eta_i=1-\frac{d_i}{D_i} \tag{11}$$

If there is no particle in the quadrat, let $d_i=D_i$, which leads to $\eta_i=0$.

The average of η_i is used to measure the entire particle uniformity with the local information. The formula is as follows:

$$I_3=\frac{1}{q}\sum_{i=1}^{q}\eta_i=\frac{1}{q}\sum_{i=1}^{q}(1-\frac{d_i}{D_i})=1-\frac{1}{q}\sum_{i=1}^{q}\frac{d_i}{D_i} \tag{12}$$

Local distance index I_3 value has limited the variation in a small range form 0 to 1 where the larger I_3 value indicates better uniformity.

With the combination of the three indices, the model of copper particle uniformity is as follows:

$$I=\sum_{i=1}^{3}w_iI_i, w_1+w_2+w_3=1, w_1\geq 0, w_2\geq 0, w_3\geq 0 \tag{13}$$

4. Experiments and Discussions

4.1. Copper Particle Detections

The copper is detected by the proposed method. Three samples are used in the numerical implementations. The parameters used in the experiments are as follows: TEM image is divided into 10×10 sub-images; the structuring element of morphological closing and opening was a square element with four pixels as its width. Figure 3 illustrates the particle detection results. Figure 3(a) shows the TEM images for sample A. Figure 3(b) and (c) represent the sample B and C, respectively. Figure 3(d)-(f) show the results image processing, where the area threshold in noise reduction is s_A=100, s_B=100 and s_C=100. It could be found that the particle size change little due to small structuring element. Figure 3(g)-(i) show the position of the particles, where the red stars represent the centroid of the particles. It could be seen that the algorithm performs well. Hence, the particle number, size and position are reliable.

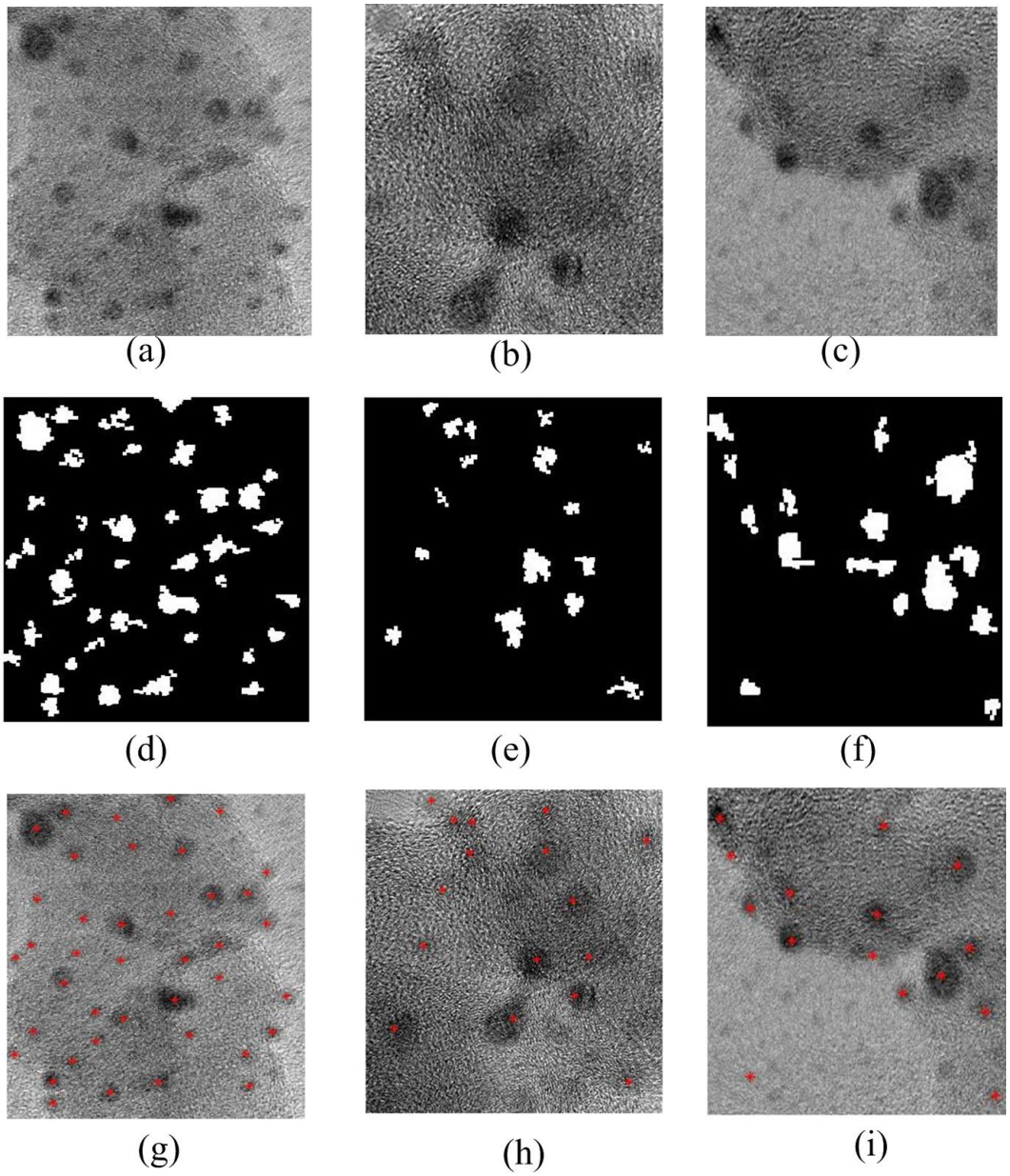

Figure 3: Results of Copper Particle Locations through Image Processing

Table 1 presents the data provided by the experiment result on particle location. The option is to use a set of well-known metrics for quantitative evaluation purposes, including hits, missed and false. Hits denote the number of correct detections. Missed means the particle is not detected. False represents false detections. It could be seen from the table that the accuracy is more than 93%, which also indicates the effective of our approach. Meanwhile, it is sufficient to quantify the uniformity of copper particles based on the detection results.

Table 1: The Detection Result Of Copper Particles

Sample	Particle number	Hits	Missed	False	Location accuracy (%)
A	41	40	1	1	97.56
B	17	16	0	1	94.12
C	16	15	1	1	93.75

4.2. Particle Quantifications

In this part, TEM image is divided into 2×2 quadrats. The particle number and size in each quadrat can be achieved by the following steps.

If the kth particle centroid belongs to the ith quadrat, let $S_{k,i}= S_{k-1,i}+a_k$, $N_{k,i} = N_{k-1,i}+1$.

Where, $S_{k,i}$ denotes the overall size of particles in the ith quadrat. a_k is the size of the kth particle. $N_{k,i}$ is the particle number in ith quadrat. Hence, our database is established. Figure 4 illustrates the data collection method. It can be found that the blue boundaries pass through some particles. Hence, it is obvious to decide the quadrat holding the particle by the centroid of the particle. It also shows that the local uniformity affects the entire uniformity by the particle size, number and position, which mean the proposed model is reasonable.

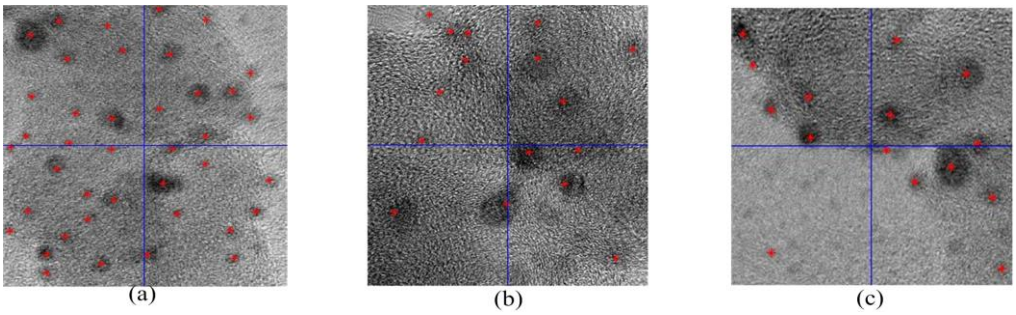

Figure 4: Data Collections with the Quadrat Number *Q=4*

The histograms of particle number and size distribution are illustrated in Figure 5. From the subjective judgment, it could be found that sample A holds the best uniformity, sample B takes the second uniformity, and sample C has the lowest uniformity. It is the similar situations to the particle size distribution. From the objective aspects, the standard deviation is $\sigma_A = 1.41$, $\sigma_B = 1.63$ and $\sigma_C = 1.89$ in the number distributions. Meanwhile, $\sigma_A = 355.87$, $\sigma_B = 342.76$ and $\sigma_C = 932.63$ are captured in the size distributions. It is mostly the same to visual achievement. It is worth to notice that $\sigma_A > \sigma_B$ in the number distribution, while $\sigma_A < \sigma_B$ in the size distribution. Hence, it can be concluded that only using one index to quantify the uniformity is unreasonable.

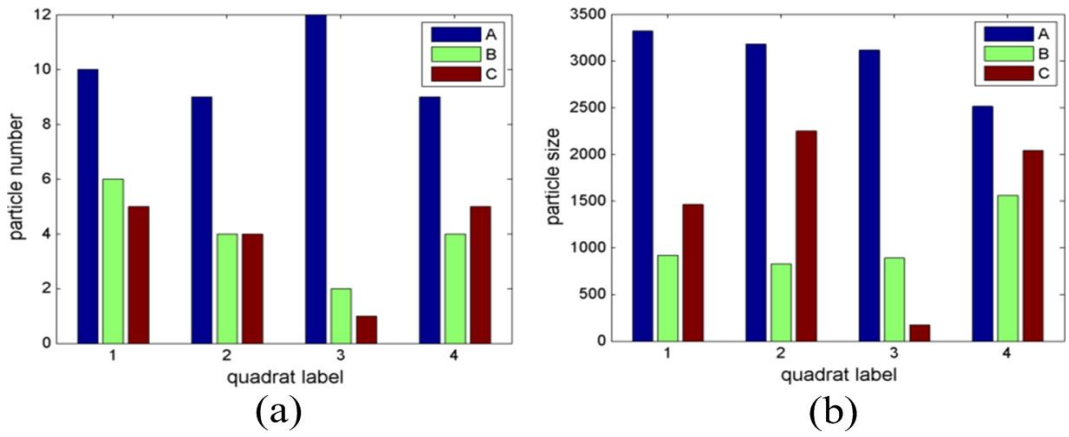

Figure 5: Distributions of Particle Size and Number with *Q=4*

4.3. Uniformity Quantification With Different Quadrat Number

Experiments are implemented with the proposed uniformity model. The weight of each index is chosen to be *1/3*. Firstly, sample A is used to verify the performance of the proposed method. Then, we compare the three samples with the changing quadrat number. Finally, it is suggested to use the average uniformity to represent the particle uniformity.

Figure 6 shows the uniformity quantification results of sample A. In figure 6(a), it can be seen that the uniformity is reduced with the growth of quadrat number. The reason is that there are so many particles are on the quadrat boundaries that the indices cannot reflect the actual situation of the particle uniformity. Hence, the quadrat number should be low. Figure 6(b) shows the uniformity results with the deferent index. It can be found the quadrat number has the most influence on the local distance index. The other two indices also reduced with the growth of quadrat number. Therefore, it can be concluded that all the indices are sensitive to the quadrat number. Currently, it is difficult to restrain the sensitive of the indices. It also implies that the quadrat number should be low.

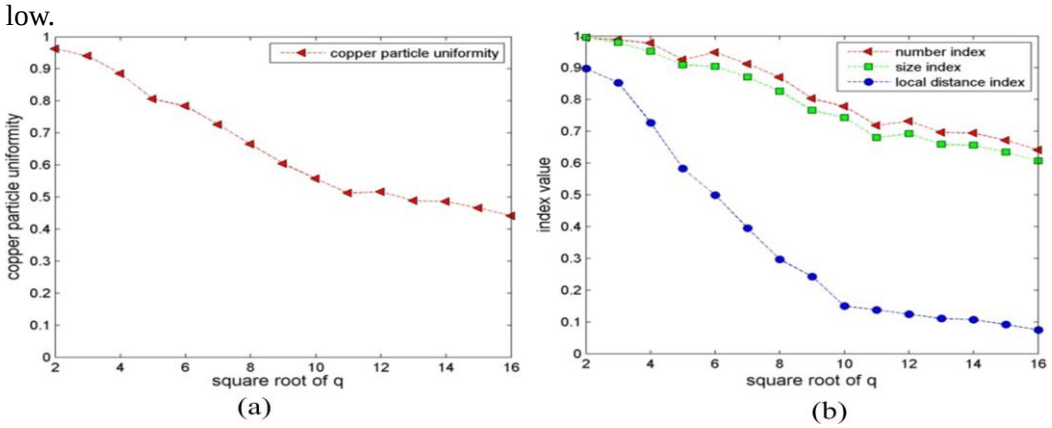

Figure 6: Uniformity Quantifications with Q from 4 to 256.

Based on the aforementioned, the quadrat number varies from 4 to 36. Figure 7 shows the comparisons of the three samples. From figure 7(a), it can be seen the sample A holds the best uniform. Sample B has the better uniformity than the sample C. Hence, it is consistent with visual achievement. Now, it can be concluded the proposed model is effective. It is apparent that all the indices of sample A have the best uniform (see figure 7(b)-(d)). However, the indices in sample B and sample C have the intersection, which

indicates the uniformity of sample B and sample C should use all the indices for the comparison. It is more satisfactory with the implementation of the spatial information.

To get more dependable uniformity results and to eliminate the impact of image processing error, average of the first *n* uniformity is noted as the final uniformity of the copper particles. The results are shown in Table 2. It can be found that the average uniformity is higher than the corresponding uniformity. Hence, it is implied that the average uniformity is more reliable than the uniformity calculating by a certain quadrat number.

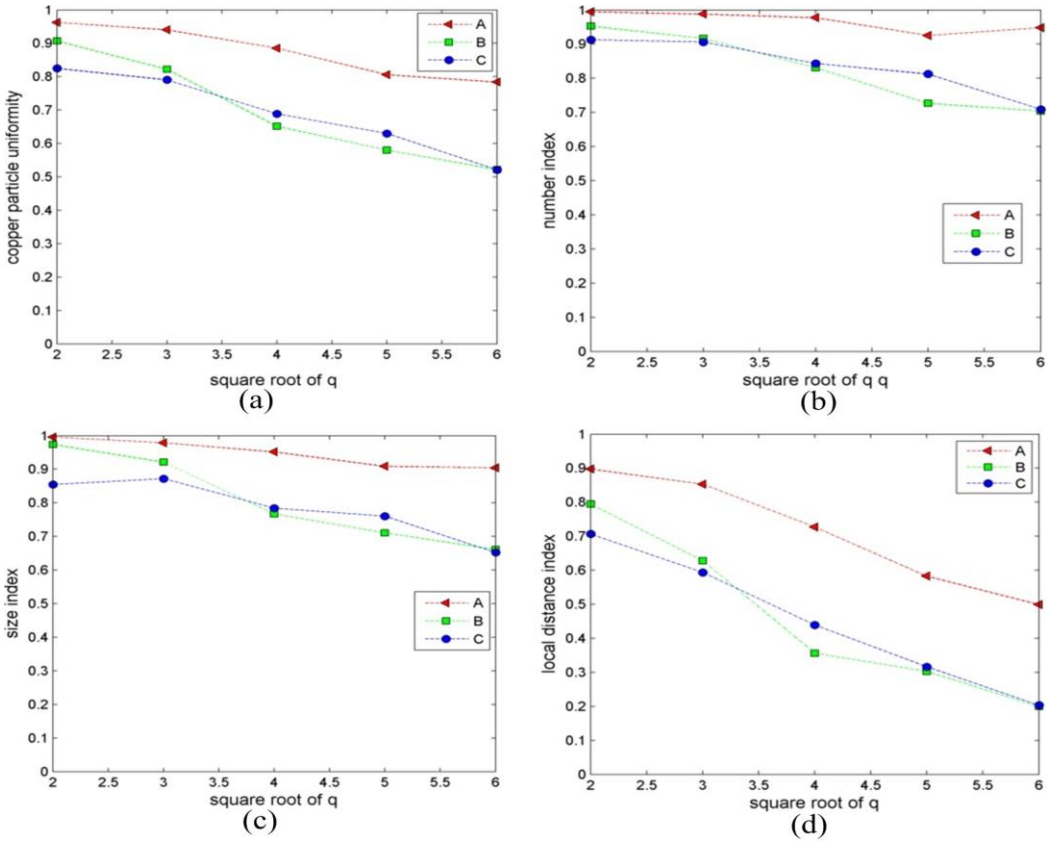

Figure 7: Calculation of Uniformity and Index Value in Figure A, B and C Corresponding To Different Quadrat Number *Q*.

Table 2: Uniformity and Average Uniformity Calculation With Quadrat Number *Q*

Sample	Uniformity with quadrat number *q*				
	q=4	*q=9*	*q=16*	*q=25*	*q=36*
A	0.9627	0.9400	0.8853	0.8056	0.7839
B	0.9069	0.8219	0.6513	0.5802	0.5215
C	0.8247	0.7906	0.6889	0.6298	0.5214
	Average uniformity				
	First one	First two	First three	First four	First five
A	0.9627	0.9513	0.9293	0.8984	0.8755
B	0.9069	0.8644	0.7934	0.7401	0.6964

C	0.8247	0.8076	0.7681	0.7335	0.6911

5. Conclusions

In this paper, an image-based method for uniformity quantification in formulation design is proposed, where the copper-coated graphite is used as the experiment material. The findings are as follows.

Firstly, the accuracy of particle location is more than *93%* location accuracy based on the clustering algorithm. Hence, the database is robust to the noise and the background. Secondly, the advantage of the proposed uniformity model is the combination of particle size, number and its local spatial information. It shows more information of the particle is used in the proposed model. Hence, the result is more reasonable than the conventional model.

Thirdly, quantifying the particle uniformity using the average uniformity is more reliable than only using a certain quadrat number to quantify the uniformity. Meanwhile, the quadrat number should be low in the quadrat methods based on the results of uniformity evaluation with the changing quadrat number.

Finally, according to the above-mentioned conclusions, the proposed model is effective to quantify the uniformity of particles, and the proposed method can be easily extended to other quality control systems.

Acknowledgments

The authors would like to acknowledge the valuable contribution of Miao-miao Tan and Professor Ping Hu. Tan collected the data and made the specimens that are used in the paper. Discussing with them, we have a better understanding of the significance of the study.

References

[1] J. X. Wang, R. J. Zhang, J. Xu, C. Wu and P. Chen, “Effect of the content of ball-milled expanded graphite on the bending and tribological properties of copper-graphite composites”, Materials and Design, vol.47, **(2013)**, pp.667-671.
[2] D. L. Saums and R. A. Hay, “Developments for Copper-Graphite Composite Thermal Cores for PCBs for High-Reliability RF Systems”, 8th International Conference on Integrated Power Systems (CIPS), vol.1, **(2014)**, pp.25-27.
[3] Z. L. Hu, Z. H. Chen, J. T. Xia and G. Y. Xia, “Properties of electric brushes made with Cu-coated graphite composites and with copper powders”, Trans. Nonferr. Met, Soc. China, vol.17, **(2007)**, pp. s1060-s1064.
[4] A. Guillet, E. Yama Nzoma and P. Pareige, “A new processing technique for copper-graphite multifilamentary nanocomposite wire: microstructures and electrical properties”, Journal of Materials Processing Technology, vol.182, **(2007)**, pp.50-57.
[5] L. Zeng, Q. Zhou, M. De Cicco, X. Li and S. Zhou, “Quantifying boundary effect of nanoparticles in metal matrix nanocomposite fabrication processes”, IIE Transactions, vol.44, **(2012)**, pp.551–67.
[6] K. M. Kama, L. Zeng, Q. Zhou, R. Tranc and J. Yang, “On assessing spatial uniformity of particle distributions in quality control of manufacturing processes”, Journal of Manufacturing Systems, vol.32, **(2013)**, pp.154-166.
[7] N. A. C. Cressie, Editor, Statistics for spatial data Revised Edition. New York, John Wiley &Sons, **(1993)**.
[8] L. I. Tong, C. H. Wang and D. L. Chen, “Development of a new cluster index for wafer defects. Int J Adv Manuf Technol”, vol.31, (2007), pp.705–715.
[9] C. H. Chena, P. J. Tsaiaa and C. Y. Lai. “Effects of uniformities of deposition of respirable particles on filters on determining their quartz contents by using the direct on-filter X-ray diffraction (DOF XRD) method”, Journal of Hazardous Materials, vol. 176, (2010), pp.389-394.
[10] G. J. Zhao, "Test on Evaluation Index of Deformation Performance for Polyester Fiber Reinforced Asphalt Concrete”, 2010 International Conference on Intelligent System

Design and Engineering Application (ISDEA), vol. 2, (2010), pp.561-564.
[11]M. Vaezi, V. Pandey, S. Bhattacharyya, "Lignocellulosic biomass particle shape and size distribution analysis using digital image processing for pipeline hydro-transportation", Biosystems Engineering, 114, (2013), pp.97-112.
[12]M. Sezgin and B. Sankur, "Survey over image thresholding techniques and quantitative performance evaluation", Journal of Electronic Imaging, vol.13, (2004), pp.146-165.
[13]T. W. Ridler and S. Calvard, "Picture thresholding using an iterative selection method", IEEE Trans. Syst. Man Cybern, SMC-8, (1978), pp.630-632.
[14]J. Guan, T. X. Zhang, X. P. Wang and J. J. Mei, "New class of Grayscale Morphological Filter to enhance infrared building target", IEEE Aerospace and Electronic Systems Magazine, vol.27, (2012), pp.5-10.
[15]M. Camesasca, M. Kaufman and I. Manas-Zloczower, "Quantifying fluid mixing with the Shannon entropy", Macromolecular Theory and Simulations, vol.15, (2006), pp.595-607.
[16]A. Guida, A.W. Nienow and M. Barigou, "Shannon entropy for local and global description of mixing by Lagrangian particle tracking", Chemical Engineering Science, vol.65, (2010), pp.2865-2883.

Authors

Hai-Ming Liu, he received the B.S. degree in Information and Computing Science from the Wuhan University of Technology, China, in 2009. He received the M.S. degree from the Applied Mathematics from Wuhan University of Technology, China, in 2012. Currently, he is PhD candidate in Mechanics department at Wuhan University of Technology. His research interests include intelligent control, image processing and machine learning.

Email ： hmliu@whut.edu.cn

Zhang-Can Huang, he received the B.S. degree in Applied Mathematics from Jilin University, China, in 1983. He received the PhD degree in Software and Computer Theory from Wuhan University. He is a professor in intelligent control and evolutionary computation. He has published over 70 papers in high quality journals and conferences. Currently, his research interests include intelligent transportations, computer vision and optimization.

Email ： huangzc@whut.edu.cn